Nanoscale

Accepted Manuscript

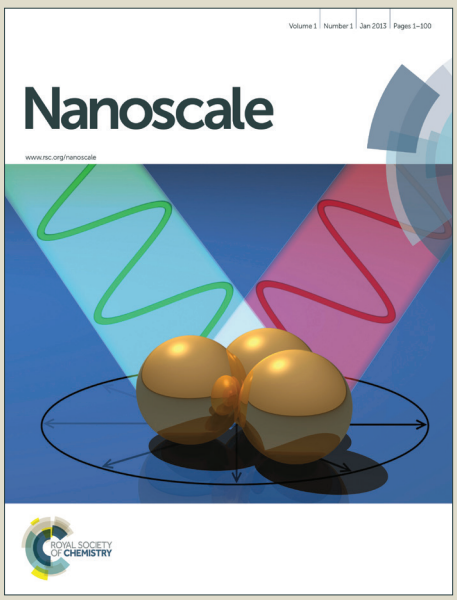

ROYAL SOCIETY OF CHEMISTRY

www.rsc.org/nanoscale

Deep Localized Distortion of Alternating Bonds and Reduced Transport of Charged Carriers in Conjugated Polymers under Photoexcitation

Cong Wang,[a] De-Yao Jiang,[a] Ren-Ai Chen,[b] Sheng Li*[a,b,c] and Thomas F. George*[c]

[a] *Department of Physics, Zhejiang Normal University, Jinhua, Zhejiang, 321004, P. R. China. E-mail: shenglee@zjnu.cn*

[b] *Department of Physics, Fudan University, Shanghai, 200433, P. R. China.*

[c] *Office of the Chancellor and Center for Nanoscience, Departments of Chemistry & Biochemistry and Physics & Astronomy, University of Missouri–St. Louis, St. Louis, Missouri, 63121, USA. E-mail: tfgeorge@umsl.edu*

In a real bulk heterojunction polymer solar cell, after exciton separation in the heterojunction, the resulting negatively-charged carrier, a polaron, moves along the polymer chain of the acceptor, which is believed to be of significance for the charged carrier transport properties in a polymer solar cell. During the negative polaron transport, due to the external light field, the polaron, which is re-excited and induces deep localization, also forms a new local distortion of the alternating bonds. It is revealed that the excited polaron moves more slowly than the ground-state polaron. Furthermore, the velocity of the polaron moving along the polymer chain is crucially dependent on the photoexcitation. With an increase in the intensity of the optical field, the localization of the excited polaron will be deepened, with a decrease of the polaron's velocity. It is discovered that, for a charged carrier, photoexcitation is a significant factor in reducing the efficiency during the charged carrier transport in polymer solar cells. Mostly, the deep trapping effect of charged carrier in composite conjugated polymer solar cell presents an opportunity for the future application in nanoscale memory and imaging devices.

1. Introduction

During the past 30 years, there has been tremendous effort to develop efficient organic solar cells.[1-9] This started with investigations of small organic molecules.[2,3,9] Meanwhile, with the development of semiconducting polymers, their application to organic solar cell gave rise to significant improvements of this field.[4,5,8,10] The first generation of organic solar cells was fabricated like a sandwich, where the center of the cell is a single organic layer inserted between two metal electrodes.[2,3] The power conversion efficiencies of such implementation were low, and even the best performance was only 0.7%.[11,12] In 1986, Tang improved the power conversion efficiency to 1%. In his approach, the single organic layer was replaced by two organic layers, forming an organic bilayer heterojunction.[13] Since then, the derivatives of such a solar cell based on double organic layers have been reported to gain higher power conversion efficiencies.[14] In 1992, Sariciftci *et al.* observed that within only 100 fs, photoinduced electron efficiently transfers from a conjugated polymeric donor to the fullerene-based acceptor, leading to the invention of the polymer-fullerene bilayer heterojunction solar cell.[15-19]

The process of converting light into electricity in an organic solar cell can be divided into four basic steps: (a) In the presence of an external light field, an electron in the photoactive layer is excited due to absorption of a photon, resulting in an electron-hole pair or an exciton. (b) The exciton diffuses towards the interface between the donor and acceptor. (c) At the interface, the exciton is dissociated into an electron and a hole. Afterwards, the electron departs from the donor and enters the acceptor, whereas the hole still resides in the donor. (d) As free charge carriers, the electron and hole move towards the cathode and anode, respectively. The above process can be 'labeled' as exciton formation, exciton diffusion, exciton separation and charge carrier transport.

For achieving an efficient organic solar cell, it is desirable to improve the efficiency of each step mentioned above. Given spontaneous transition or non-radiative transition triggering the exciton decay during the exciton diffusion process, one of the general approaches is to reduce the exciton diffusion length. The layout of a bulk heterojunction is thus proposed for the morphological reason. Its internal structure consisting of a well-organized bulk heterojunction is depicted in Fig. 1,[20] where the donor and acceptor are of a fine mixture.[21,22] However, this well-organized morphology of bulk heterojunction is hard to fabricate at the nano-scale. In general, conjugated polymers – one-dimensional-morphological acceptors – are dissolved in the

donor domain to form a realistic bulk heterojunction solar cell, whose layout is sketched in Fig. 2.

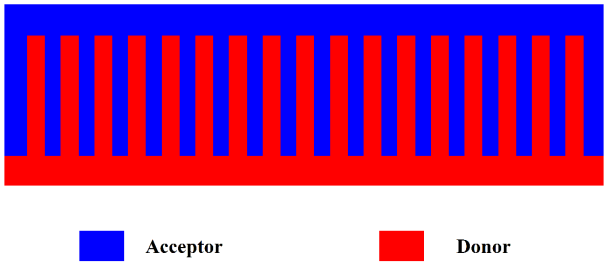

Fig. 1 Diagrammatic cross-section of the ideal morphology of a bulk heterojunction solar cell.

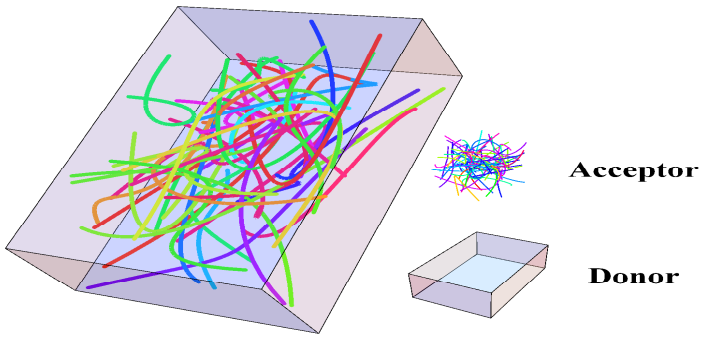

Fig. 2 Diagrammatic layout of a bulk heterojunction solar cell in 3D.

Due to this structure, the heterojunction randomly fills the whole space, which also greatly improves the possibility that due to the interface distributed all over the bulk of solar cells, once a photon is absorbed, an exciton or electron-hole pair is formed and is separated, even omitting or shortening the step of exciton diffusion, which reduces the exciton decay because of diffusion.

Indeed, in phase-separated blend films of regioregular P3HT (RR-P3HT) and PCBM, it is found that most excitons can be dissociated into free polarons efficiently after almost all of them reach the interface of RR-P3HT/PCBM.[23] Besides the charged polarons from the dissociation of the exciton, ultrafast spectroscopic measurements clearly show an increased polaron pair yield for higher excess energies directly after photoexcitation when compared to the exciton population.[24] For charged carriers in a conjugated polymer, it seems possible that there also exist new doubly-charged carriers, i.e., bipolarons. In 2011, Raman spectroscopy exhibited the transformation of bipolarons into polaron pairs in long oligothiophene dications, where the

formation of biradical polaron pairs marks the end of the quinoidal stability promoted by the intrinsic proaromatic character. [25] Thus, after the exciton separation, charge carrier transport, as the following step, is actually the transport of polarons.

In a real bulk heterojunction solar cell, the resulting charged carrier-polaron moves along the polymer chain of the acceptor. As compared to the distance in a bulk heterojunction of ideal morphology in Fig. 1, the layout of real bulk heterojunction, as shown in Fig. 2, extends over the distance for charge carrier transport, although it reduces the length for exciton diffusion. This means that there exists a long distance for charged carrier migration in a polymeric molecule before the charged carrier arrives at the cathode and anode. Therefore, an investigation of charged carrier transport in a one-dimensional conjugated polymer chain is particular significant for revealing the properties of the bulk heterojunction solar cell, which is one of the issues addressed in this paper.

As for the factors determining the transport of charged carriers in conjugated polymers, it is suggested that, based on experimental observation, the charge carrier mobility in conjugated polymers is determined by two factors. One is charge transfer integrals between monomer units due to molecular wire planarization. A more important factor is the reduction of energetic disorder.[26] Besides, it also raises a puzzle as to whether there exists other underlying factors working on the transport of polarons. Considering the long-distance transport of charged polarons, it can be assumed that under the influence of an external light field, the charged carrier can readily be excited when moving along an acceptor polymer. More importantly, the assumption is validated by a recent experiment where photoexcitation leads to deep localization of free electrons photogenerated from composite P3HT/PC60BM NPs at the NP/dielectric interface and hole trapping by fullerene anions in composite P3HT/PC60BM NPs.[27] Further, it provides a possible mechanism that photoexcitation can re-excite a charged carrier in the conjugated polymer, such as a polaron, and then induce deep localized distortion of the lattice structure, which also leads to an another important issue in this paper as to how a charged carrier is excited and transports in a one-dimensional conjugated polymer chain before reaching the anodes.

Thus, by incorporating the conventional molecular dynamics with the time-dependent electron transition process under photoexcitation, this paper aims to deepen the understanding of charged carrier motion under an external optical field in photovoltaic devices based on

conjugated polymers, in particular, organic bulk heterojunction solar cells. The deep trapping effect of charged carriers in a composite conjugated polymer solar cell presents an opportunity for future applications in nanoscale memory and imaging devices.

2. Methodology

Let us consider a conjugated polymer undergoing external photoexcitation, with an electron making a transition from a down-level Γ_d to an up-level Γ_u. In regard to Γ_u, let $|u\rangle$ represent its wave function, E_u its energy value, and P_u its electron population. Correspondingly for Γ_d, we have $|d\rangle$, E_d, and P_d. Photon absorption occurs on the condition that the photon energy is identical to the band gap between Γ_u and Γ_d. Within the time span Δt, the change of population ΔP_u consists of two parts: one is ascribed to a stimulated transition, $\Delta P_{d\to u}$, and the other to a spontaneous transition, $\Delta P_{u\to d}$:

$$\Delta P_u = \Delta P_{d\to u} + \Delta P_{u\to d} \quad . \tag{1}$$

Without the restriction of Pauli repulsion, the dipole moment between Γ_u and Γ_d can be written as $p = \langle u|r|d\rangle$, where r is the dipole operator in the polymer chain. Then the stimulated transition rate can be expressed as a function of light field of frequency ω and energy density ρ as

$$W_{d\to u} = \frac{4\pi^2}{3\hbar^2} p^2 \rho(\omega)\delta(\omega - \frac{E_u - E_d}{\hbar}) \quad . \tag{2}$$

As for spontaneous emission, the spontaneous transition rate $\gamma_{u\to d}$ between these states is determined by

$$\gamma_{u\to d} = \frac{4(E_u - E_d)^3}{3\hbar^4 c^3} p^2 \quad . \tag{3}$$

By means of the stimulated transition rate together with spontaneous transition rate, the change of population in levels Γ_u and Γ_d can be expressed as

$$\Delta P_{d\to u} = W_{d\to u} P_u \Delta t \text{ , and } \quad \Delta P_{u\to d} = -\gamma_{u\to d} P_u \Delta t \quad . \tag{4}$$

Therefore, due to an electron transition, the evolutions of the electron populations P_u and P_d are expressed by the decay equation

$$\lim_{t\to 0} \frac{\Delta P_u}{\Delta t} = \lim_{t\to 0} \frac{\Delta P_{d\to u} + \Delta P_{u\to d}}{\Delta t} = \frac{dP_{u\to d}}{dt} = (W_{d\to u} - \gamma_{u\to d}) P_u$$

$$P_d = n - P_u \tag{5}$$

where n is the total electron number. Thanks to the above equations, combined with the molecular dynamics, the motion of a polaron along a one-dimensional conjugated polymer chain can be completely described.

As for the one-dimensional conjugated polymer chain, it is described by the well-known Su-Schreiffer-Heeger model with an additional part that includes the electric field. Considering electron-phonon and electron-electron interactions together with the elastic potential energy of lattice, the Hamiltonian for the conjugated polymer can be expressed as

$$H = H_{e-p} + H_{e-e} + H_l + H_{el}$$

$$H_{e-p} = -\sum_{l,s}[t_0 + \alpha(u_{l+1} - u_l) + (-1)^l t_e] \times [c^{\dagger}_{l+1,s} c_{l,s} + c^{\dagger}_{l,s} c_{l+1,s}]$$

$$H_{e-e} = U \sum_{l} n_{l,\uparrow} n_{l,\downarrow} + V \sum_{l,s,s'} n_{l,s} n_{l+1,s'}$$

$$H_l = \frac{K}{2} \sum_{l} \left(u_{l+1} - u_l\right)^2$$

$$H_{el} = \sum_{l} Ee \left(l - \frac{N+1}{2} \right) a n_{l,s}, \tag{6}$$

where t_0 is an intrachain hopping constant (2.5~5.0 eV), α denotes an electron-lattice coupling constant (4.78 eV/Å), $c^{\dagger}_{l,s}$ ($c_{l,s}$) stands for the electron creation (annihilation) operator with spin s at the l^{th} monomer with displacement u_l, and t_e is the Brazovskii-Kirova term (0.05~0.12 eV). K is an elastic constant (21 eV/Å^2). U (2.0~5.0 eV) and V (0.5~2.0 eV) are the on-site and nearest-neighbor Coulomb interactions, respectively, and a is the lattice constant (1.22~3.5 Å). E (10^{-3}~5×10^{-2} mV/ Å) is strength of the electric field.

The electron's behavior can be derived from its energy spectrum ε_μ and wavefunction $\Phi_\mu = \{Z^s_{l,\mu}\}$, which are functionals of the time-dependent lattice displacement u_l, as determined by the eigenequation,

$$H\Phi_\mu = \varepsilon_\mu \Phi_\mu \tag{7}$$

The electron-electron interaction is treated in the Hartree-Fock approximation, so that the above eigenequation can be rewritten as follows:

$$\varepsilon_\mu Z^s_{l,\mu} = \left[U\left(\rho_l^{-s} - \frac{1}{2} \right) + V(\sum_{s'} \rho^{s'}_{l-1} + \sum_{s'} \rho^{s'}_{l+1} - 2) \right] Z^s_{l,\mu}$$
$$-[V\sum_{\mu}^{occ} Z^s_{l,\mu} Z^s_{l-1,\mu} + t_0 + \alpha(u_{l-1} - u_l) + (-1)^{l-1} t_e] Z^s_{l-1,\mu} \quad (8)$$
$$-[V\sum_{\mu}^{occ} Z^s_{l,\mu} Z^s_{l+1,\mu} + t_0 + \alpha(u_{l+1} - u_l) + (-1)^{l+1} t_e] Z^s_{l+1,\mu}$$

The charge distribution is defined as $\rho^s_l = \sum_{\mu}^{occ} | Z^s_{l,\mu} |^2 - n_0$, where n_0 is the density of the positively-charged background.

Considering that atoms are much heavier than electrons, the atomic displacement of the l^{th} monomer can be described classically using the Feynman-Hellmann theorem. Thus the dynamic equation can be written as

$$M \frac{d^2 u_l}{dt^2} = -\sum_{\mu}^{occ} \frac{\partial \varepsilon_\mu}{\partial u_l} + K(2u_l - u_{l+1} - u_{l-1}), \quad (9)$$

where occ denotes the occupation of electrons. The one-dimensional polymer chain in our calculation is of finite length with fixed ends. Using the above coupled equations and conventional molecular dynamics, we can quantitatively describe the dynamical evolution of not only the electronic states but also the lattice structure in a conjugated polymer chain.

3. Results and discussion

In polymeric solar cell, a photoinduced exciton is separated into charged carriers at the donor-acceptor interface. For the convenience of our calculation, a conjugated polymer chain consisting of 200 units is used as the acceptor of the heterojunction interface. After photoinduced exciton fission, a negatively-charged carrier-polaron occurs in the polymer chain. During the process, Fig. 3 describes the evolution of the energy levels of orbitals near the energy gap, where the levels near LUMO and HOMO are marked in blue Fig. 3(a) and (b), respectively, while the evolution of the LUMO and HOMO levels is displayed in green. We see that energy levels of both LUMO and HOMO leave from the original states to become localized in the center of energy gap. For a simple representation, we rename the original LUMO and HOMO as Γ_u and Γ_d. The schematic picture for the evolution of electron-acceptor system is illustrated as Fig. 4.

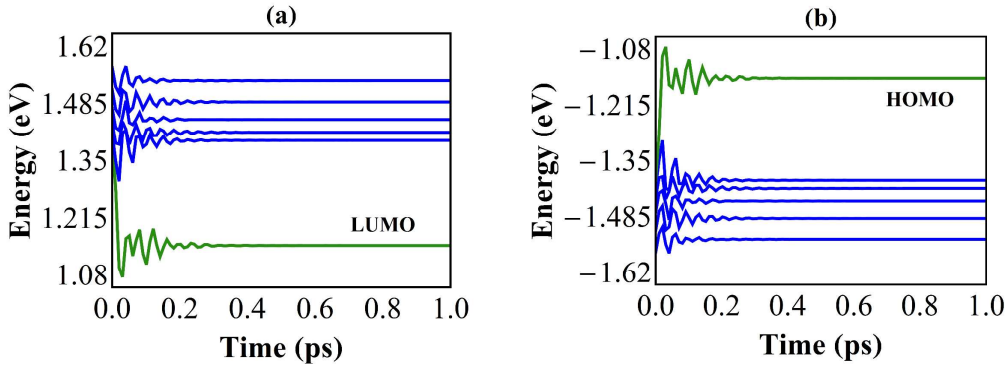

Fig. 3 Evolution of the energy levels of orbitals near LUMO (a) and HOMO (b).

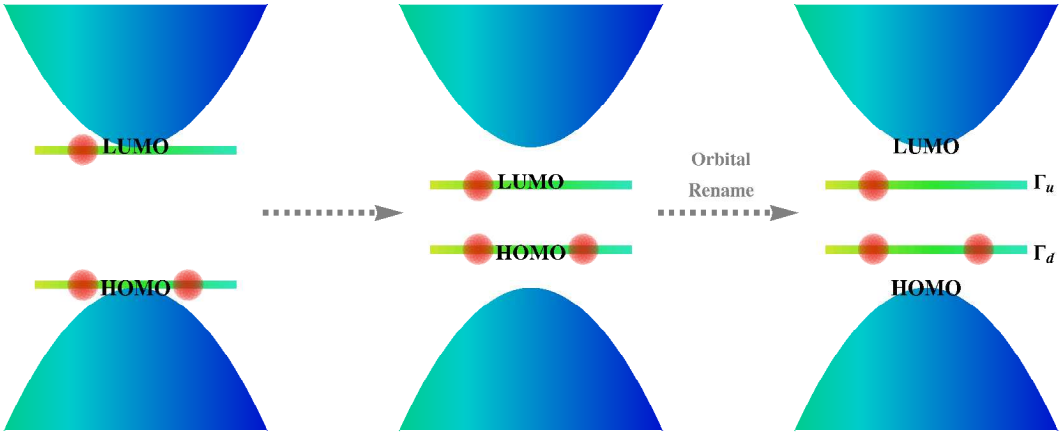

Fig. 4 Schematic picture for the formation of localized orbitals in the band gap.

The charged carrier transported in the polymer acceptor is regarded as a polaron.[28] Considering the electron-phonon interaction of the conjugated polymer, the formation of the polaron leads to the distortion of the alternating bonds, which can be described by the displacement of units u as shown in Fig. 5. Here the absolute values of the displacement of the units are mostly above 0.05 Å but fall below 0.05 Å at the center of the polymer chain, which is attributed to localization caused by the negative polaron. Recasting the value of an atomic displacement in terms of color, we visualize the distortion in the conjugated polymer chain in Fig. 6 for the range of the polymer chain chosen between the 70th and 130th lattice unit sites. The distortion represented by a different color pattern is found around the 100th lattice site, namely the center of the polymer chain.

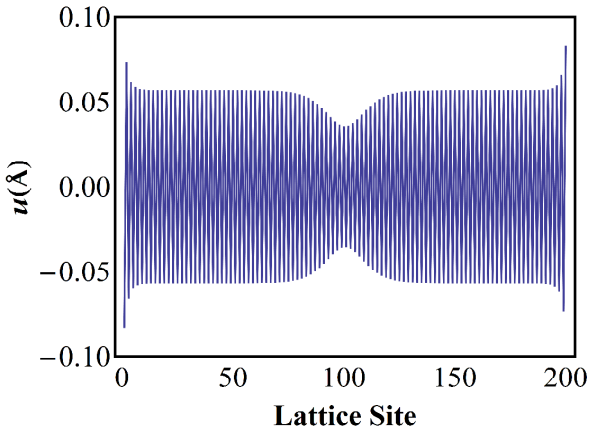

Fig. 5 Atomic displacement at each lattice site.

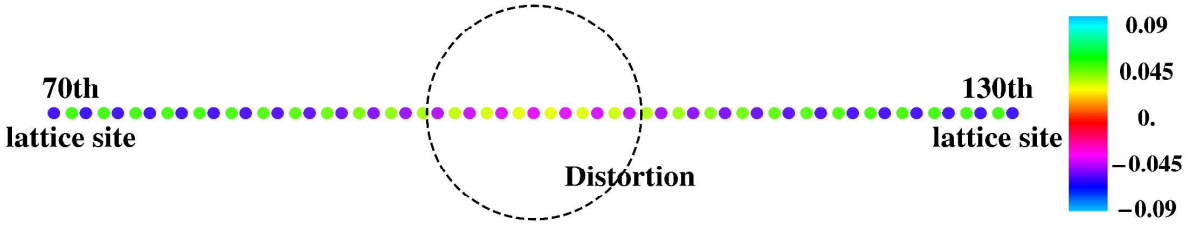

Fig. 6 Color representation of the distortion in a one-dimensional conjugated polymer chain.

Upon application of an electric field, the negatively-charged polaron will move along the conjugated polymer chain in the opposite direction of the electric field. To describe its dynamics, we see that the polaron initially stays around 50th lattice site, where polymer chain is made up of 200 lattice sites. The position of the polaron is obtained by probing its charge. Within the time window of 400 fs, the electric field then drives the negative polaron to move to around the 150th lattice site. This is depicted in Fig. 7, where the site location of the polaron is in a linear relation with time.

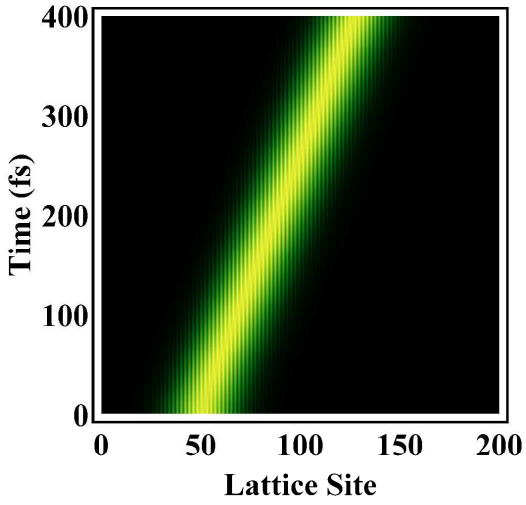

Fig. 7 Time-dependent polaron motion under an electric field without photoexcitation.

We now consider the motion of a polaron under the influence of both an electric field and an optical field, where the latter induces photoexcitation. A two-step process for the polaron motion is shown in Fig. 8(a), where in the first step without photoexcitation, the polaron moves linearly in time from the 50^{th} to the 100^{th} lattice site within first 200 fs, with an average velocity of ~ 0.25 site/fs. For the second step from 200 to 1000 fs, an optical field of intensity 20 $\mu J/cm^2$ is applied to excite the polymer chain, leading to a remarkably slow polaron motion. Let us now change the intensity of the optical field to 0.2 $\mu J/cm^2$ at 200 fs, where we see in Fig. 8(b) that the excited polaron moves more quickly than in the case of 20 $\mu J/cm^2$. Here the transport begins around the 90^{th} lattice site and finishes around 175^{th} site within the a 800 fs time interval. Its average velocity is approximately 0.11 site/fs slower than that of the polaron without photoexcitation. As a result, the previous hypothesis is partially valid that the slower motion results from the photoexcitation, as validated in Fig. 8.

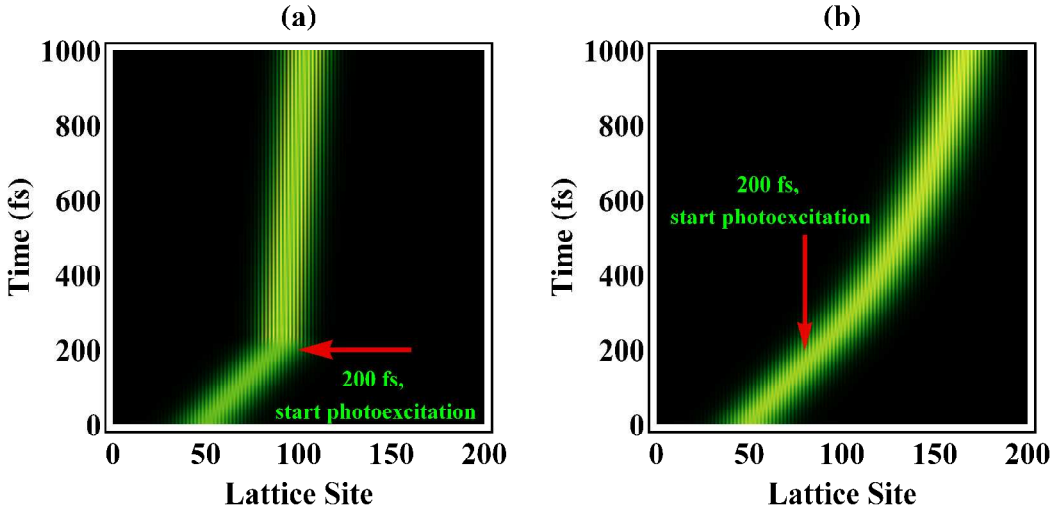

Fig. 8 Polaron motion along the lattices with respect to time under an electric field, where photo-photoexcitation with 20 μJ/cm^2 (a) and 0.2 μJ/cm^2 (b) is added after 200 fs.

To understand the reason for this phenomenon, let us consider the internal structure of the polaron by looking at the distortion of the alternating bonds, as visualized in Fig. 9. The results in the top two rows are obtained within the first 200 fs, thus describing the polaron transport without photoexcitation. As demonstrated in Fig. 9(a,c), up to 200 fs, the polaron moves over nearly 50 lattice sites, and its size and span of distortion remains about the same, although the position changes. At 200 fs, an optical field of 20 μJ/cm^2 is applied to trigger photoexcitation of the polaron. Distortion of the alternating bonds of the excited polaron is more dramatic, as seen in Fig. 9(e,g). For better clarification, on the right panel of Fig. 9, the localized distortion of the polaron is displayed by the red color on the background of the non-distorted alternating bonds marked in blue and green. As we can see from the right panel (as well as the left), the local distortion in Fig. 9(f,h) moves more slowly than indicated in Fig. 9(b,d), indicating that the velocity of excited polaron decreases.

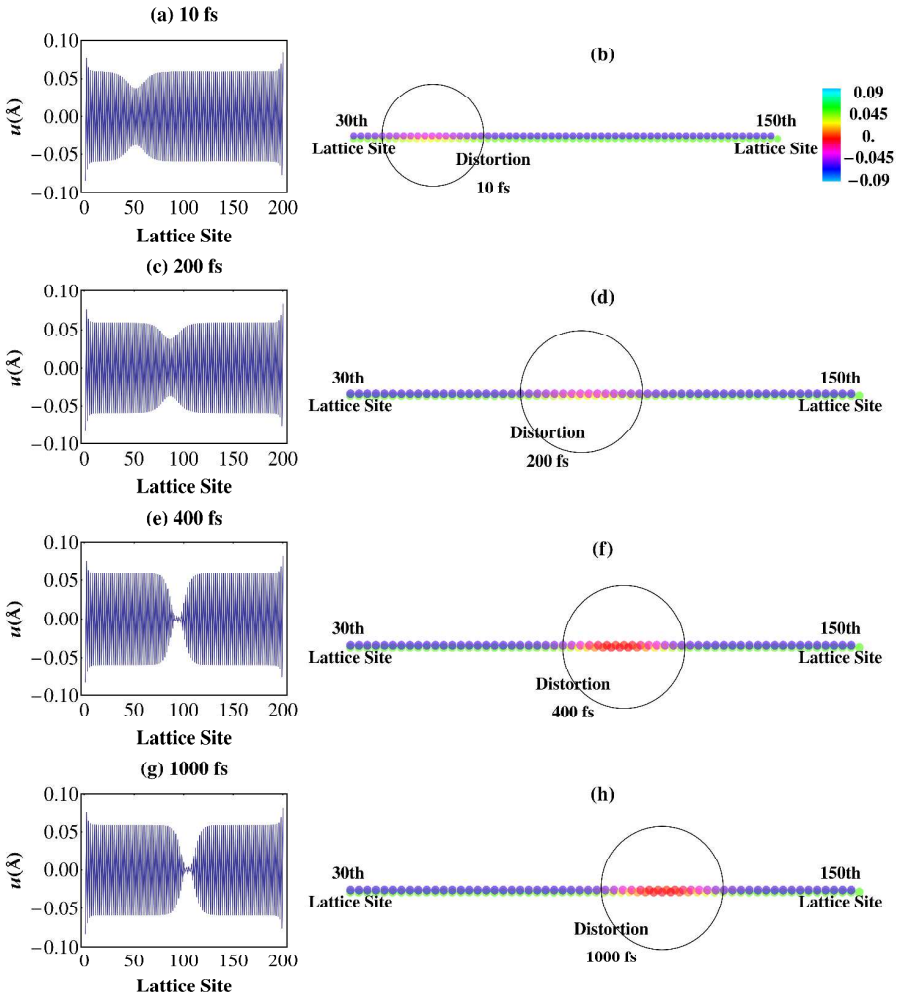

Fig. 9 Evolution of atomic displacement (left panel) of a conjugated polymer chain and its visualized representation in colors (right panel), observed at 10 fs, 200 fs, 400 fs, and 1000 fs, due to photoexcitation by the optical field of intensity 20 μJ/cm2 after 200 fs.

Let us now consider the negative polaron is driven by an electric field and an optical field of intensity 0.2 μJ/cm^2 on the polymer acceptor, whose evolution is illustrated in Figure 10. As with our discussion of Fig. 9, the top two rows depict the motion of the polaron up to 200 fs without photoexcitation, i.e., due only to the driving electric field. After the optical field is applied to excite the polaron, Fig. 10(g,h) shows that although the excited polaron moves more slowly than in the ground state, it transports more quickly than the polaron excited by the optical field of intensity 20 μJ/cm^2. Comparing Fig. 10(e) with 10(a,c), we see that the alternating bonds of the negative polaron are slightly distorted.

As demonstrated in Figs. 9 and 10, the velocity of the polaron moving along the conjugated

polymer chain essentially depends on the amount of distortion of the alternating bonds. Thus, the more photoexcitation distorts the alternating bonds bond, the more slowly the polaron moves. Also, this provides an explanation for the nonlinear curve of the motion of polaron in Fig. 8(b), where the velocity of motion is instantaneously changing with photoexcitation as long as the polaron enlarges the distortion of the alternating bonds.

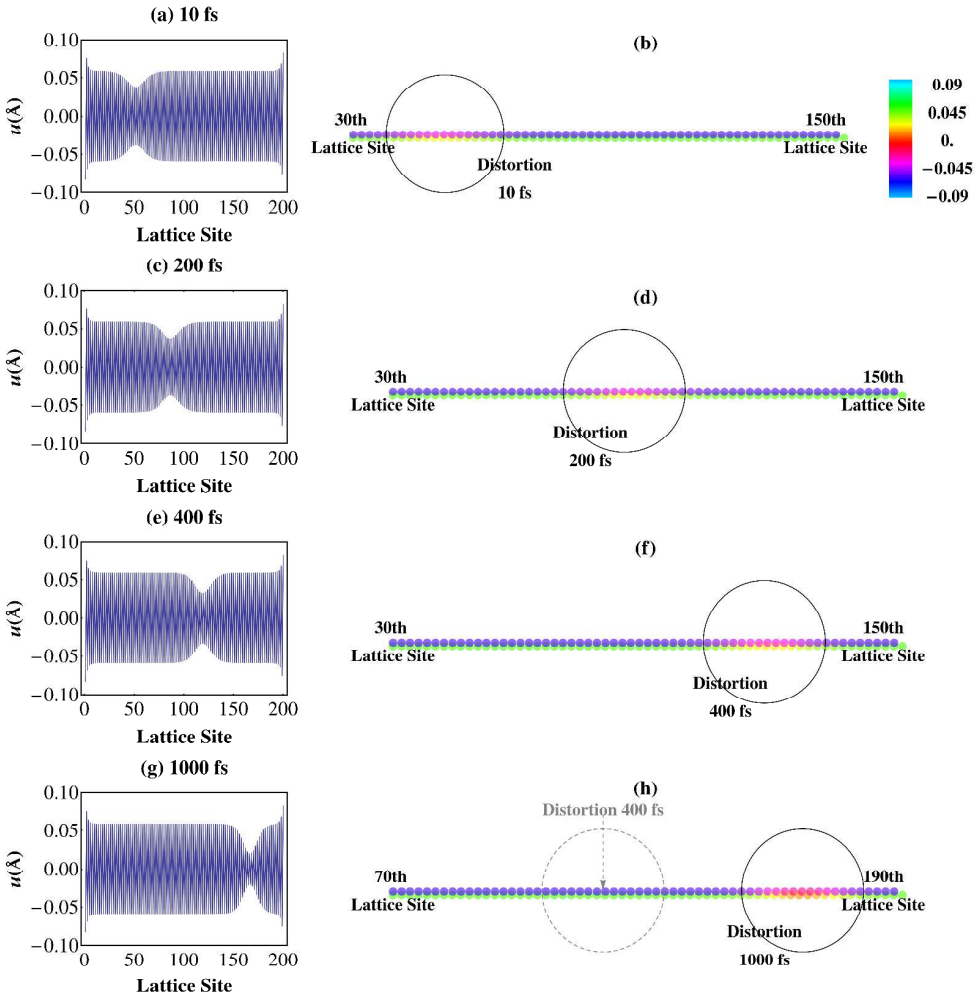

Fig. 10 Evolution of atomic displacement (left panel) of a conjugated polymer chain and its visualized representation in colors (right panel), observed at 10 fs, 200 fs, 400 fs, and 1000 fs, due to photoexcitation by the optical field of intensity 0.2 μJ/cm^2 after 200 fs.

4. Conclusions

In a real bulk heterojunction solar cell, after exciton separation in the heterojunction, the resulting negatively-charged carrier-polaron moves along the polymer chain of the acceptor.

During the negative polaron transport, thanks to the external light field, the polaron is re-excited, leading to a new local distortion of the alternating bonds. A comparison of the transport properties of the ground-state polaron with those of a photoexcited polaron reveals that the excited polaron moves more slowly than the ground-state polaron. Further, with an increase of the intensity of the external optical field, the distortion of the alternating bonds of the excited polaron becomes significant, slowing down the velocity of the excited polaron. As a result, the transport properties of an excited charge carrier are concluded to be smaller compared to the ground-state case, indicating a defect that reduces the efficiency of organic solar cells.

Acknowledgments

This work was supported by the National Science Foundation of China under Grant 21374105, the Zhejiang Provincial Science Foundation of China under Grant R12B040001, and the public project of Zhejiang province under Grant 2014C31135.

References

1 G. A. Chamberlain, *Solar Cells*, 1983, **8**, 47–83.
2 Woührle and D. Meissner, *Adv. Mater.*, 1991, **3**, 129–138.
3 C. J. Brabec, N. S. Sariciftci, and J. C. Hummelen, *Adv. Funct. Mater.*, 2001,**11**,15–26.
4 J. Nelson, Curr. Opin. *Solid State Mater. Sci.*, 2002, **6**, 87–95.
5 Y. Li and Y. Zou, *Adv. Mater.*, 2008, **20**, 2952–2958.
6 G. Dennler, M. C. Scharber and C. J. Brabec, *Adv. Mater.*, 2009, **21**, 1323–1338.
7 C. Li, M. Liu, N. G. Pschirer, M. Baumgarten and K. Müllen, *Chem. Rev.*, 2010, **110**, 6817–6855.
8 A. Facchetti, *Chem. Mater.*, 2011, **23**, 733–758.
9 C. Piliego and M. A. Loi, *J. Mater. Chem.*, 2012, **22**, 4141–4150.
10 C. Winder and N. S. Sariciftci, *J. Mater. Chem.*, 2004, **14**, 1077–1086.
11 D. L. Morel, A. K. Gosh, T. Feng, E. L. Stogryn, P. E. Purwin, R. F. Shaw and C. Fishman, *Appl. Phys. Lett.*, 1978, **32**, 495–497.
12 A. K. Gosh and T. Feng, *J. Appl. Phys.*, 1978, **49**, 5982–5989.
13 C. W. Tang, *Appl. Phys. Lett.*, 1986, **48**, 183–185.
14 M. Hiramoto, M. Suezaki and M. Yokoyama, *Chem. Lett.*, 1990, **19**, 327–330.

15 N. S. Sariciftci, L. Smilowitz, A.J. Heeger and F. Wudl, *Science*, 1992, **258**, 1474–1476.

16 L. Smilowitz, N. S. Sariciftci, R. Wu, C. Gettinger, A. J. Heeger and F. Wudl, *Phys. Rev. B*, 1993, **47**, 13835–13842.

17 C. H. Lee, G. Yu, D. Moses, K. Pakbaz, C. Zhang, N. S. Sariciftci, A. J. Heeger and F. Wudl, *Phys. Rev. B*, 1993, **48**, 15425–15433.

18 S. Morita, A. A. Zakhidov and K. Yoshino, *Solid State Commun.*, 1992, **82**, 249–252.

19 S. Morita, S. Kiyomatsu, X .H. Yin, A .A. Zakhidov, T. Noguchi, T. Ohnishi and K. Yoshino, *J. Appl. Phys.*, 1993, **74**, 2860–2865.

20 C. Y. Yang and A. J. Heeger, *Synth. Met.*, 1996, **83**, 85–88.

21 M. C. Scharber and N. S. Sariciftci, *Prog. Polymer Sci.*, 2013, **38**, 1929–1940.

22 G. Yu, J. Gao, J. C. Hummelen, F. Wudl and A. J. Heeger, *Science*, 1995, **270**, 1789–1791.

23 J. Guo, H. Ohkita, H. Benten and S. Ito, *J. Am. Chem. Soc.*, 2010, **132**, 6154–6164.

24 R. Tautz, E. D. Como, C. Wiebeler, G. Soavi, I. Dumsch, N. Fröhlich, G. Grancini, S. Allard, U. Scherf, G. Cerullo, S. Schumacher and Jochen Feldmann, *J. Am. Chem. Soc.*, 2013, **135**, 4282–4290.

25 S. R. González, Y. Ie, Y. Aso, J. T. L. Navarrete and J. Casado, *J. Am. Chem. Soc.*, 2011, **133**, 16350–16353.

26 A. A. Kocherzhenko, S. Patwardhan, F. C. Grozema, H. L. Anderson and L. D. A. Siebbeles, *J. Am. Chem. Soc.*, 2009, **131**, 5522–5529.

27 Z. Hu and A. J. Gesquiere, *J. Am. Chem. Soc.*, 2011, **133**, 20850–20856.

28 P. B. Miranda, D. Moses and A. J. Heeger, *Phys. Rev. B*, 2001, **64**, 81201.